Extended Range Electric Vehicle With Driving Behavior Estimation in Energy Management

Korosh Vatanparvar, *Graduate Student Member, IEEE*, Sina Faezi, *Graduate Student Member, IEEE*, Igor Burago, *Graduate Student Member, IEEE*, Marco Levorato, *Member, IEEE*, and Mohammad Abdullah Al Faruque, *Senior Member, IEEE*

***Abstract*—Battery and energy management methodologies have been proposed to address the design challenges of driving range and battery lifetime in Electric Vehicles (EV). However, the driving behavior is a major factor which has been neglected in these methodologies. In this paper, we propose a novel context-aware methodology to estimate the driving behavior in terms of future vehicle speeds and integrate this capability into EV energy management. We implement a driving behavior model using a variation of Artificial Neural Networks (ANN) called Nonlinear AutoRegressive model with eXogenous Inputs (NARX). We train our novel context-aware NARX model based on historical behavior of real drivers, their recent driving reactions, and route average speed retrieved from Google Maps in order to enable driver-specific and self-adaptive driving behavior modeling and long-term estimation. We analyze the estimation error of our methodology and its impact on a battery lifetime-aware automotive climate control, comparing to the state-of-the-art methodologies for various estimation window sizes. Our methodology shows only 12% error for up to 30-second speed prediction which is an improvement of 27% compared to the state-of-the-art. Therefore, the higher accuracy helps the controller to achieve up to 82% of the maximum energy saving and battery lifetime improvement achievable in ideal methodology where the future vehicle speeds are known.**

***Index Terms*—CPS, Electric Vehicle, Battery, HVAC, Energy Management, Statistical Modeling, Neural Network, Model Predictive Control, Optimization.**

I. Introduction and Related Work

ELECTRIC VEHICLES (EV) have been introduced as a zero-emission method of transportation to address environmental issues such as air pollution [1]. However, major design challenges in EV have affected their economy and sustainability thereby hindering their development process [2]. Battery as the main energy source in the EVs introduces design challenges especially for applications with stringent design constraints. For instance, weight, cost, and volume design constraints restrict the energy stored in the EV limiting the driving range. Moreover, battery capacity diminishes under utilization, degrading the battery lifetime [3]. Furthermore, the rate-capacity effect reduces the available battery capacity for higher discharge rates resulting in a worse driving range [4].

The electric motor is a major component in the EVs that consumes energy in the motor mode and generates energy in the regenerative mode when braking. Future reactions of the driver in terms of adjustments to vehicle direction and speed, based on the driver's perception of the route and vehicle condition are described as driving behavior. The energy consumption/generation depends on the driving behavior on the route and can vary for different drivers [5, 6] (see Figure 1). Moreover, other accessories in EVs especially Heating, Ventilation, and Air Conditioning (HVAC) system have shown to be another major contributor to battery energy consumption [7–10]. The HVAC energy consumption depends on its utilization and the ambient temperature, thereby making HVAC a flexible load. The total power request in the EV influences the battery operating behavior and will be illustrated in EV driving range and battery lifetime that are the major EV design challenges [11].

Design challenges in EVs have been addressed by designing more efficient and robust battery cells, device-level Battery Management Systems (BMS), or system-level battery and energy managements. The device-level methodologies monitor or control the cells in order to maintain their safe and efficient operation [12]. Moreover, as we focus in this paper, system-level methodologies are implemented to optimize the battery utilization by adjusting higher-level power requests in order to improve the battery lifetime and driving range [13, 14].

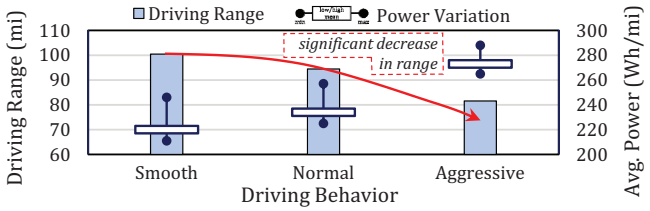

Fig. 1. Impact of different driving behavior on EV power consumption variation and driving range tested on Nissan Leaf [5].

For instance, it has been shown that the driving route influences the EV energy, thereby the EV driving range and battery lifetime (see Figure 1). This is in addition to the fact that the driving route also affects driving time and distance. Hence, navigation systems have been implemented to optimize and select the best route for a specific EV [15–18]. In another work, route prediction has helped in optimizing the energy split between battery and ultracapacitor in Hybrid Electrical

Manuscript received June 16, 2017; revised September 26, 2017; accepted February 4, 2018.

This material is based upon work partially supported by the National Science Foundation under Grant No. ECCS 1611349.

K. Vatanparvar, S. Faezi, and M. A. Al Faruque are with the Department of Electrical Engineering and Computer Science, University of California, Irvine, Irvine, CA 92697, USA (e-mail: kvatanpa@uci.edu; sfaezi@uci.edu; alfaruqu@uci.edu).

I. Burago and M. Levorato are with the Department of Computer Science, University of California, Irvine, Irvine, CA 92697, USA (e-mail: iburago@uci.edu; levorato@uci.edu).

Energy Storage (HEES) [1, 4]. Furthermore, a battery lifetime-aware automotive climate control has been implemented which considers the driving route in the future to predict the EV power requests and optimize the HVAC operation while maintaining passenger thermal comfort [8–10].

The above-mentioned system-level battery and energy management methodologies require information regarding the future EV power requests for optimizing the control inputs. Hence, they have assumed that the driving route - which can be provided by the navigation system - is known before hand for estimating future EV states. However, the driving route is not the only factor affecting the EV power. The driving behavior of a driver regarding the driving route condition is also influential. Experiments have been conducted to illustrate how driving behavior affects the power consumption.

Motivational case study on driving behavior: the impact of different aggressiveness levels of driving behavior on the EV power has been analyzed using historical data. Figure 1 shows the power consumption and estimated driving range evaluated for a Nissan Leaf simulated in FASTSim [5, 6].

Summary and conclusion from observations: we realized that the driving behavior may significantly affect the EV acceleration and speed, and thereby the power consumption. Hence, the driving behavior should be accounted into the energy management as well. However, current EV power prediction has been limited to the knowledge of only the driving route. This limitation significantly decreases the estimation accuracy required for the EV battery and energy managements.

Driving behavior modeling has been investigated and exploited for driver assistant systems, especially for vehicle safety purposes [19, 20]. These models attempt to eliminate the driver's decision-making lag of 0.5-1.5 seconds [21, 22] and predict the future reactions up to a few seconds. For instance, in the state-of-the-art modeling methodologies using Hidden Markov Model (HMM), Neural Network (NN), and graph modeling, the driver's behavior in terms of the vehicle speed is predicted up to the next 3 seconds with accuracy of up to 99.5% [23–25]. These controllers need to be triggered within a few seconds before an event for safety purposes. Hence, we consider their prediction as short-term ($<$ 5 seconds). However, these short-term predictions are not sufficient for battery and energy management methodologies. They require more accurate and longer-term predictions of at least more than 5 seconds to perform well. The requirement for longer prediction time is mainly due to the fact that the physical process involved is much slower. We consider their prediction as long term when the prediction time is comparable to the duration of driving segments.

A. Problem and Research Challenges

The problem of driving behavior modeling and estimation for EV energy management poses the following challenges:

1) Energy and battery managements in EV do not account driving behavior for optimization, although it affects the EV operating parameters - driving range and battery lifetime.
2) Accuracy of the EV power consumption estimation has been at stake due to lack of driving behavior consideration.
3) Driving behavior modeling methodologies focus only on very recent input information and current state (visible environment around the car) for short-term prediction. This leads to failure of the prediction for longer period of time.

B. Main Contributions and Concept Review

To address the above-mentioned challenges, a novel methodology of driving behavior modeling and estimation for EV energy management is proposed which employs:

1) **Electric Vehicle Modeling (Section II-A):** main EV components such as electric motor, HVAC, and battery are modeled using Ordinary Differential Equations (ODE) and operating parameters such as power consumption and battery lifetime are estimated for various driving conditions.
2) **Driving Behavior Modeling (Section II-B):** driving behavior is modeled using a variation of Artificial Neural Networks (ANN) by training a novel context-aware Nonlinear AutoRegressive model with eXogenous Inputs (NARX) [26, 27] based on historical behavior of the drivers, their recent reactions, and the average speed of the route reported by Google Maps. This context-aware model estimates the driving behavior of a specific driver in terms of the vehicle speed for up to 30 seconds (long term).
3) **Integration into EV Energy Management (Section III):** the estimated future maneuvers of the driver in terms of vehicle speeds are utilized in the battery and energy management methodologies for improving the battery lifetime and driving range. In this paper, a battery lifetime-aware automotive climate control is implemented and its performance has been analyzed using our novel context-aware driving behavior modeling and estimation methodology.

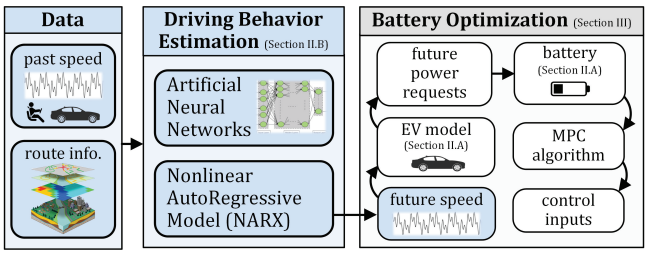

Fig. 2. Illustration of our novel context-aware driving behavior modeling and estimation for energy management (contributions highlighted).

Figure 2 illustrates our proposed methodology to estimate the driving behavior. In this paper, the EV driving dynamics are modeled given the driving behavior. Moreover, a context-aware NARX model (variation of ANN) is generated and trained using driving route information and corresponding real data of the driver's behavior. Our novel model is self-adaptive with respect to specific driver behavior and is able to predict the driving behavior for long-term up to 30 seconds. We integrate our context-aware model into a newly adjusted energy management methodologies. Hence, their control inputs are adjusted given the future vehicle speeds and EV power requests to minimize power variation, energy consumption, and extend the battery lifetime.

II. System Modeling and Estimation

Recent energy management methodologies deployed in EVs, as in the battery lifetime-aware automotive climate control, require modeling of the EV components for predicting their dynamic behavior and power requests (see Section II-A). Moreover, estimation of the driving behavior and vehicle speed (see Section II-B) is required for accurate estimation of the EV power request. The system modeling and estimation is then used for optimizing and adjusting the control inputs in order to improve the EV driving range and battery lifetime.

A. Electric Vehicle

EV as an automotive Cyber-Physical System (CPS) consists of many interconnected subsystems with various functionalities and responsibilities. There are two subsystems in EV (electric motor and HVAC) which are the main contributors to energy consumption/generation (i.e. battery utilization). Their functional behavior needs to be investigated and modeled, for estimating the EV power request at each instance of time.

Electric motor generates the necessary force to drive the vehicle. The power consumption or generation of the electric motor in the EV is modeled and estimated by considering the motor characteristics and driving forces on the vehicle such as: gravitational (F_{gr}), aerodynamic drag (F_{aero}), and rolling resistance (F_{roll}) forces.

$$F_{tr} = F_{gr} + F_{aero} + F_{roll} + ma \tag{1}$$

The tractive force (F_{tr}) is provided by the electric motor to overcome the forces to propel the vehicle with mass (m) forward at a desired speed (v) and acceleration (a) [28]. The direction of F_{tr} is defined by whether the electric motor is in regenerative mode (regenerative braking) or motor mode.

The electrical motor power consumption (P_e) is calculated as:

$$P_e = \frac{F_{tr} v}{\eta_m} \tag{2}$$

where η_m represents the electric motor efficiency when converting electrical to mechanical energy in the motor mode and converting mechanical to electrical energy in the regenerative mode (regenerative braking). η_m is dependent on the motor rotational speed and the generated torque; its values are provided as the electric motor specifications [14, 29, 30].

HVAC system is monitored and controlled by the automotive climate control to maintain the cabin temperature. The cabin temperature (T_z) is influenced by the supply air temperature (T_s), flow rate ($\dot{m}_z$), the cabin heat capacity (M_c), and the heat capacity of the air (c_p). The relationships between these variables and parameters are defined by ordinary differential equations describing thermodynamics in the HVAC system [8].

The HVAC system power consumption consists of: 1) cooling power, 2) heating power, and 3) fan power. The cooling and heating power consumption is due to the energy difference between their inlet and outlet air flow:

$$P_c = \frac{c_p}{\eta_c} \dot{m}_z (T_m - T_c) \tag{3}$$

$$P_h = \frac{c_p}{\eta_h} \dot{m}_z (T_s - T_c) \tag{4}$$

where P_c and P_h are cooling and heating power consumption. η_c and η_h are the efficiency parameters of the cooling and heating processes. Moreover, the heat exchange between the coolant/evaporator and air is modeled as efficiency parameters. The air returned from the cabin (T_z) and the outside air (T_o) are mixed and recirculated back into the cooling coil. T_m is the temperature of the mixed air and d_r is the mixture fraction [$T_m = (1 - d_r)T_o + d_r T_z$]. T_c is the temperature of the outlet air after cooling before heating. The fan power consumption (P_f) is quadratically related to $\dot{m}_z$ and k_f is a parameter that captures the fan efficiency and the duct pressure losses.

$$P_f = k_f (\dot{m}_z)^2 \tag{5}$$

The parameters for the model are set based on an HVAC specifications and to accurately describe the thermodynamic behavior in different conditions [8, 31].

Battery provides the power requested by the EV systems such as the electric motor and the HVAC. The influence of these power requests on the battery are estimated by models of the battery operating behavior such as State-of-Charge (SoC) and battery lifetime degradation or State-of-Health (SoH).

The usable capacity inside a lithium-ion battery decreases with higher discharge rate (I) (rate-capacity effect). This effect is modeled by the Peukert's Law using the effective current. Hence, the SoC of the battery is estimated by the coulomb counting and measuring the effective discharge rate:

$$SoC^t = SoC^0 - \frac{100}{C_n} \times \int_0^t I \left(\frac{I}{I_n} \right)^{pc-1} dt \tag{6}$$

where C_n is the nominal capacity measured at nominal current (I_n) predefined by the manufacturer. SoC^t represents the SoC value at time t. pc is the Peukert's constant typically measured empirically for the type of lithium-ion battery cell [32, 33]. For the battery type used here, pc is evaluated as 1.1342. Although this constant is necessary to capture the battery consumption behavior, our methodology is not influenced by its value.

Ratio of current capacity to nominal capacity (SoH) degrades over time in lithium-ion batteries (capacity-fade effect). The SoH degradation ($\bigtriangledown SoH$) is mainly influenced by the stress on the battery cell which is modeled by SoC deviation (SoC_{dev}) and SoC average (SoC_{avg}). $\bigtriangledown SoH$ is related to the pattern of SoC values over a time period [3] following Equation 7:

$$\begin{aligned} \bigtriangledown SoH &= f\ (SoC_{dev}, SoC_{avg}) \\ &= \ (a_1 e^{\alpha SoC_{dev}} + a_2)(a_3 e^{\beta SoC_{avg}}) \end{aligned} \tag{7}$$

where α, β, a_1, a_2, and a_3 are the parameters for estimating $\bigtriangledown SoH$ accurately based on the battery type. Thorough evaluation of the battery temperature influence on $\bigtriangledown SoH$ is out of the scope of the paper. Hence, we have modeled it as a constant in Equation 7.

The EV components are modeled using the above-mentioned equations. Moreover, their parameters are extracted

from the manufacturers' forums and experimental data provided by the third-parties testing the vehicle (see Table I).

TABLE I
COMPONENTS SPECIFICATIONS OF THE NISSAN LEAF EV.

Specification		Nissan Leaf S
Battery	Energy	24 KWh
	Voltage	403.2 v
	Capacity	59.52 Ah
Body	Weight	1471 Kg
	Height	1.5494 m
	Width	1.7703 m
Wheel	Rim Diameter	16 inch
	Overall Diameter	25 inch
Gear	Single Ratio	7.9377

B. Driving Behavior

The driving forces on the vehicle are evaluated by knowing the driving behavior given the EV model (see Section II). The driving behavior depends on the driving route and reactions of the driver to specific route condition. Although the driving behavior estimation is leveraged in the battery optimization, they operate independently of each other. In the following, we describe state-of-the-art methodologies to model the driving behavior in terms of the future vehicle speed that will be used for EV power request prediction in the battery optimization:

1) Ideal (IDL). In this model, we are able to predict the vehicle speed at any given time with perfect accuracy. In other words, a controller would have access not only to the previous and current vehicle speeds, but also to the future vehicle speeds.

2) Motion-Preserving (MP). Typically, in rule-based or optimization-based methodologies [34, 35], either there is no assumption about the future, or the assumption is that the vehicle is going to preserve its current motion. In other words, in this model, the future vehicle speed after h seconds, is assumed to be determined by the following physics-based equation,

$$v_{t|k} = v_{t|0} + a_{t|0} \times k \tag{8}$$

where $v_{t|0}$ and $a_{t|0}$ are the speed and acceleration values at time t. $v_{t|k}$ is the speed for time $t+k$ predicted at time t.

3) Statistical Modeling. In this approach, the future vehicle speed is predicted using past speeds, current speed, and information of any other factors that can affect the vehicle speed. Since the correlation between the current speed and predicted speed decreases for further future time instances, the estimation error increases. In order to address this, as part of our novel methodology, statistical information of the average speed for each road segment ($\widetilde{v}$) extracted from Google Maps APIs [36] is also fed to the model providing the future context and condition of the driving route. Given the current location of the vehicle, the future trajectory of the vehicle and the average speed values can be determined using the map database. The average speed at a specific time is a feature and information that is provided that can represent and model the uncertainty, route condition and traffic of a segment. Therefore, accounting them into the model will further reduce the prediction error. More features can be used to improve the accuracy, however, the available data of the route is limited.

To model and predict the driving behavior, we evaluate $V_t^{+h} = \{v_{t|k} : 1 \leqslant k \leqslant h\}$, which are the predicted values of the vehicle speeds for the next $h \geqslant 1$ future seconds at time t. The problem of statistical modeling is formulated as a challenge to estimate the function f in Equation 9,

$$V_t^{+h} = f\ (V_t^{-d}, \widetilde{V}_t^{-d'}, \widetilde{V}_t^{+h'}) + E_t^{+h} \tag{9}$$

where $V_t^{-d} = \{v_\tau | t-d \leqslant \tau \leqslant t-1\}$ and $\widetilde{V}_t^{-d'} = \{\widetilde{v}_\tau | t-d' \leqslant \tau \leqslant t-1\}$ represents the values for the past d and d' real speeds and average speeds before time t. $\widetilde{V}_t^{+h'} = \{v_{t|k} : 1 \leqslant k \leqslant h'\}$ represent the values for the future h' average speeds since time t. $E_t^{+h} = \{e_\tau | t+1 \leqslant \tau \leqslant t+h\}$ represent the error introduced to the system due to other factors influencing the future speeds (V_t^{+h}) such as weather, etc. However, other influencing factors have been considered to be the same for all the data and are avoided in the modeling and estimation. Hence, $\hat{V}_t^{+h} = \hat{f}\ (V_t^{-d}, \widetilde{V}_t^{-d'}, \widetilde{V}_t^{+h'})$ is predicted using $\hat{f}$, the approximation of function f. We have investigated three machine learning and modeling techniques for approximation: Random Forests, FeedForward Neural Network, and NARX.

3.a) Random Forests (RF). Multiple regression Decision Trees (DT) are combined to make an RF [37]. Each of these regression decision trees chooses a random set of input variables (features such as past, current speeds, and future average speeds) and works independently on a subset of data to model a particular aspect of the driving behavior. In a regression decision tree, instead of making deterministic decisions in the leaves as in a binary decision tree, a statistical distribution model specifies the probability of each output value. Singular decision trees easily over fit the training data. However, this is addressed in RF by randomly selecting the input features for each decision tree and combining the results. A single probability distribution is generated by weighted averaging of the probability distribution outputs of the trees based on the frequency of occurrence of a particular driver behavior in the training data set. The most probable value of the final distribution is reported as the final result of the random forests.

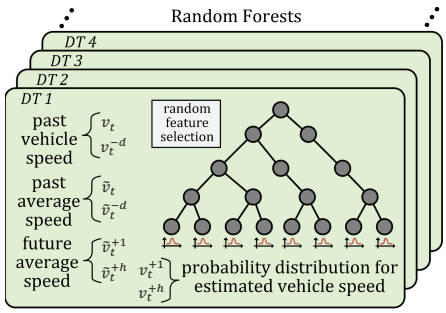

Fig. 3. RF architecture to predict each of the future speed values.

3.b) FeedForward Neural Network (FFNN). Artificial Neural Networks (ANN) are a family of models that are mostly used to estimate nonlinear functions with large number of inputs and outputs. They consist of connected artificial neurons which mimic biological neural network behavior under different topologies. In order to model driving behavior and estimate future vehicle speed (approximate function $\hat{f}$), considering lim-

ited processing power, we initially chose FFNN, the simplest, fastest, and the most common variation of ANNs [38, 39]. In an FFNN architecture, neurons in one layer are connected via directed weighted edges to only the neurons in their adjacent layer and there is no interconnection between neurons inside one layer. Moreover, as the name FFNN suggests, there are no feedback edges in this architecture of neurons (see Figure 4).

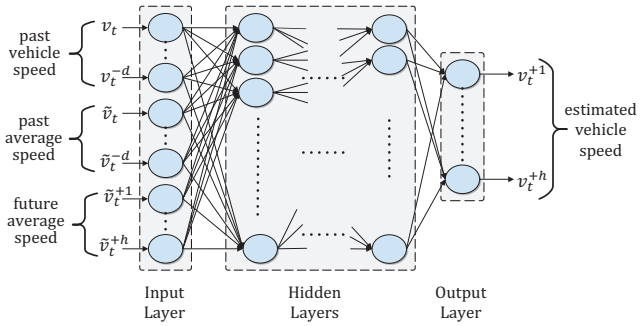

Fig. 4. FFNN architecture to predict future speed values.

The output signal of neuron i in layer $l+1$ is calculated by:

$$z_i^{l+1} = f\ (w_{0i}^l + \sum_{j=1}^{n^l} w_{ji}^l z_j^l) \tag{10}$$

where n^l is the number of neurons in layer l, w_{ji}^l is the weight of the edge between neuron j in layer l and neuron i in layer $l+1$, and w_{0i}^l is the inherent threshold of neuron i in layer $l+1$ (treated as a normal weight with the input signal being one). f is a transfer function which is (typically) chosen to be a logistic sigmoid function, $f(x) = \frac{1}{1+e^{-x}}$. Weight of the edges are calculated by a Back Propagation (BP) algorithm [40] to train the model and minimize the following performance function:

$$MSE = \frac{1}{P}\sum_{p=1}^{P}\sum_{k=1}^{K}(d_k^p - o_k^p)^2 \tag{11}$$

where *MSE* is the global mean sum squared error between the estimated outputs o^p and the targets d^p where p and k are indices for the training sample p and for the component k of the output vector, respectively.

3.c) Nonlinear AutoRegressive model with eXogenous Inputs. NARXs are one of the simplest architectures of Recurrent Neural Networks (RNN) that includes feedback edges between two different layers of nodes. RNNs are a very promising family of Neural Networks which have the capability to adapt to changes in the input/output, and typically they are much more stable in compare to FFNNs. In this work, we have choosen to focus on NARXs which inherit the adaptivity properties of their architecture family and have been proven to carry out good results in long-term prediction applications [26, 27].

As shown in Figure 5, the architecture is similar to FFNN's and the only difference is that the output of the architecture is connected to its input by a delay of one-second. In other words, to train a NARX-based model, function $\hat{f}$ in $\hat{V}_t^{+h} = \hat{f}\ (V_t^{-d}, \widetilde{V}_t^{-d'}, \widetilde{V}_t^{+h'}, \hat{V}_{t-1}^{+h})$ is estimated to minimize the effect of E_t^{+h} in Equation 9. The feedback loop in this architecture helps in capturing the behavior of a specific driver. It needs to

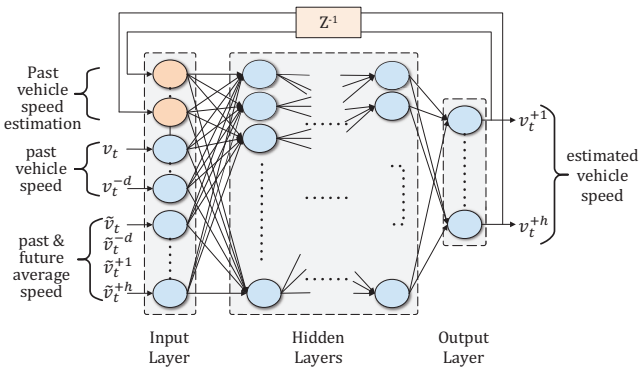

Fig. 5. NARX architecture to predict future speed values.

be noted that the NARX model adapts to the specific driver behavior at the training phase (offline) with no extra time spent online. In other words, the pre-trained NARX model has the ability to adapt its output to each individual driver's behavior, at the cost of a limited amount of processing power thanks to the feedback from its estimated outputs to its inputs.

Although RFs are known to easily achieve high accuracy for a wide range of problems, ANNs can be more accurate if their parameters are tuned for the given problem. Moreover, NARXs, as a fast recurrent architecture of ANNs, are more suitable for time-series prediction since they can memorize and utilize the recent observations in the time-series data. It needs to be noted that any technique that can reach the same accuracy is also applicable to our methodology. In this paper, our context-aware NARX model with 8 layers is used to predict 30 seconds ($h = 30$) of future vehicle speeds. The number of input features is $d = 35$, $d' = 5$, and $h' = 35$ (total 76 features). These values were decided based on the data and validation error to avoid over fitting.

III. Driving Behavior Integration with Energy Management

We elaborated on how our methodology models and estimates the driving behavior in terms of the future vehicle speeds (Section II-B). The estimated future values of the vehicle speed are used by the battery and energy managements in order to predict the EV power requests and optimize their control inputs. In this paper, we consider a battery lifetime-aware automotive climate control as an example of how to deploy this driving behavior estimation for improving the driving range and battery lifetime while maintaining the thermal comfort for the passengers. It needs to be noted that any control methodology that uses the future driving behavior for its optimization purpose can benefit from our model.

As detailed in Algorithm 1, our driving behavior modeling methodology implemented as the function $\hat{f}$, uses the past vehicle speeds (V^{-d}), past average vehicle speeds ($\widetilde{V}^{-d'}$), and future average vehicle speeds ($\widetilde{V}^{+h'}$) (by Google Maps) in order to estimate the future vehicle speeds ($\hat{V}^{+h}$) (line 1). The future vehicle speeds ($\overline{v}$) are derived to evaluate the future vehicle acceleration ($\overline{a}$) (lines 2-3). Moreover, the future road slopes ($S^{+h'}$) are retrieved and saved in $\overline{\alpha}$ from Google to predict the driving forces on the EV such as the gravitational

force (line 4). In line 5, the electric motor model is utilized to predict the power requests based on the driving behavior (see Section II-A). Then, the battery lifetime-aware automotive climate control implements a Model Predictive Control (MPC) (lines 6-9) that considers the pattern of the electric motor power requests to adjust HVAC control inputs and optimize its utilization. The objective of the optimization is to maintain the temperature and reduce the battery stress by decreasing the SoC deviation (Equation 12). Finally, the optimal control inputs are applied to the HVAC (lines 10-11).

Algorithm 1: Driving Behavior Integration with Climate Control

Input: past vehicle speeds V^{-d}
Input: past average vehicle speeds $\widetilde{V}^{-d'}$
Input: future average vehicle speeds $\widetilde{V}^{+h'}$
Input: future road slopes $S^{+h'}$
Input: current state T_z
Output: control inputs $[P_f, P_c, P_h]$

// estimate future vehicle speeds
1 $\hat{V}^{+h} \leftarrow \hat{f}\ (V^{-d},\ \widetilde{V}^{-d'},\ \widetilde{V}^{+h'})$
2 $\overline{v} \leftarrow \hat{V}^{+h}$ // future vehicle speed
3 $\overline{a} \leftarrow d\hat{V}^{+h}/dt$ // future vehicle acceleration
4 $\overline{\alpha} \leftarrow S^{+h'}$ // future road slope
// predict electric motor power consumption
5 $P_e \leftarrow$ **electric motor** $(\overline{v}, \overline{a}, \overline{\alpha})$
/* define state variables and control inputs */
6 $x^0 \leftarrow T_z$ // initial cabin temperature
7 $z \leftarrow [x, i, u, x^+]'$ // control window variables
8 **init** c_{eq}, c_{neq}, c // define constraints, cost func.
9 $\widetilde{z} \leftarrow$ **optimize** (z, c_{eq}, c_{neq}, c) // call optimizer
10 $[P_f, P_c, P_h] \leftarrow \widetilde{z}$ {*control inputs*}
11 **return** $[P_f, P_c, P_h]$

In the MPC optimization problem, the dynamic behavior of the EV including the HVAC, electric motor, and battery subsystems is modeled using (non-)linear equations (see Section II-A), multiple state variables $x = \{T_z, SoC\}$, control inputs $i = \{T_s, T_c, d_r, \dot{m}_z\}$, and auxiliary variables $u = \{T_m, P_h, P_c, P_f, P_e\}$. The values of these variables and inputs are estimated and evaluated for a future prediction horizon using the modeling equations. The controller utilizes an optimizer to adjust the HVAC control inputs such as heating and cooling coil temperature set points and fan speed in the prediction horizon while considering the EV power requests. The solver optimizes these variables to improve the battery lifetime, reduce the HVAC power influence, and maintain the cabin temperature around a specific target temperature. The relationships between the variables and control inputs are defined by (non-)equality constraints (C_{eq}, C_{neq}). Moreover, there are certain constraints on the control inputs and state variables of the MPC problem that should be satisfied during the optimization and control process for safe operation and stable control. The cost function for the optimization problem at time t is formulated as in Equation 12; $(T_z^{k|t} - T_{target})^2$ is the thermal comfort cost for minimizing the deviation of the temperature from target temperature (T_{target}); $T_z^{k|t}$ is the temperature for time $t+k$ predicted at time t. $(SoC^{+^{k|t}} - SoC^{k|t})^2$ is the battery SoC cost for minimizing the SoC deviation; $SoC^{k|t}$ and $SoC^{+^{k|t}}$ are the current and final SoC values for time $t+k$ predicted at time t. This function will result in extending the battery lifetime and decreasing the energy consumption for further driving range.

$$
\begin{aligned}
min.\ & \sum_{k=1}^{N} \frac{w_1}{\gamma_1} (T_z^{k|t} - T_{target})^2 + \frac{w_2}{\gamma_2} (SoC^{+^{k|t}} - SoC^{k|t})^2 \\
s.t.\ \ & C_{eq} \quad \text{discretized modeling equations [Eq. 1-6]} \\
& C_{neq} \quad \text{limits on control inputs and variables } [x, i, u] \\
& \quad \text{constrained cabin temperature } [\underline{T}_z \le T_z \le \overline{T}_z]
\end{aligned} \tag{12}
$$

The constraint on the cabin temperature already ensures the required thermal comfort by limiting the temperature variance. Hence, a higher priority is given to the battery SoC deviation in order to extend the battery lifetime and reduce the energy consumption. Therefore, we evaluate optimization coefficients (w_x and γ_x) accordingly to find the optimum solution in terms of the battery lifetime first, then thermal comfort cost.

Experiments on the HVAC system and its behavior analysis showed that $(\triangle T_z = 1°C)$ temperature variance results in an energy consumption equivalent to $(\triangle SoC = 0.04\%)$ battery SoC reduction per second on average. Hence, coefficients $(\gamma_1 = \triangle {T_z}^2 = 1)$ and $(\gamma_2 = \triangle {SoC}^2 = 0.0016)$ are evaluated to normalize the objective terms considering the range of their values. Moreover, weight coefficients $(w_1 = 0.1, w_2 = 0.128)$ are defined to prioritize each term accordingly. It needs to be noted that the values for weight coefficients are decided arbitrarily by trial and error, to ensure the desired battery performance. Furthermore, they can be adjusted by the designer's preferences for the trade-offs between battery lifetime and thermal comfort regardless of the estimation methodology.

Adjusting the constraints and the weight coefficients will help in finding the best optimal solution to the problem. However, the driving behavior estimation methodology is independent of the optimization process. Moreover, the optimization may be implemented using Sequential Quadratic Programming (SQP) to achieve better solution [8].

IV. Experimental Results and Analysis

A. Experimental Setup

The EV electric motor, HVAC, and battery subsystems are modeled and implemented in MATLAB/Simulink. The experiments are conducted using part of the SHRP 2 Naturalistic Driving Study [41] database. We use the driving data of three drivers in 17, 19, and 20 trips with duration of 3 to 138 minutes, each. The driving data is divided into training ($\approx 70\%$), validation ($\approx 15\%$), and test ($\approx 15\%$) splits. Each split is divided such that they include short, medium, and long distance trips on highway and localway areas. The training and prediction of the NARX model have been done using the "*train*" and "*predict*" functions in Neural Network toolbox of MATLAB. The optimization problem has been formulated as matrices in MATLAB and has been solved using "*fmincon*" function in Optimization toolbox. The computing platform used for the experiments has an Intel Core-i7 3770 CPU with 2.3 GHz clock frequency and 8 GB of 1600 DDR3 RAM.

The data is sampled every second and the simulation time step is considered to be one second as well. For instance,

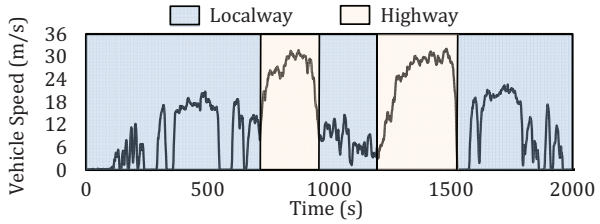

Fig. 6. Portion of the real-life vehicle speed data for two route conditions.

Figure 6 illustrates a small portion ($\approx$ 33 min = 2000 samples) of the recorded vehicle speed of a real driver that we used for training. The figure shows the behavior of the vehicle speed both in highway and localway driving areas (highlighted in the figure). These contexts are used in the training for improving the vehicle speed prediction.

B. Results and Analysis

We compare the performance of the following methodologies in terms of complexity, estimation accuracy, and resulting performance of the battery/energy optimization:

1) ***IDL:*** in ideal methodology, the values of the future vehicle speeds are known, which is the most ideal scenario.
2) ***MP:*** the vehicle is assumed to basically preserve its current motion for a specific future period. It is typically utilized for fast path prediction and collision avoidance [34, 35].
3) ***RF:*** the vehicle speed is predicted using random forests model [37] trained by real data. The future prediction is based on the past and current speed values while knowing the context of the road condition defined by the average speeds in the past and future (Section II-B).
4) ***FFNN:*** the vehicle speed is predicted using an FFNN architecture with 8 layers [38] trained by real data. The prediction is based on the past and current speed values while knowing the context of the road condition defined by the average speeds in the past and future (Section II-B). This architecture does not have any feedback loop which limits the ability to adapt to a specific driver behavior.
5) ***NARX:*** our novel context-aware modeling is implemented using an 8-layer nonlinear autoregressive model with exogenous inputs [26, 27] trained by real data. The prediction is based on the past and current speed values while knowing the context of the road condition defined by the average speeds in the past and future (Section II-B). The feedback loop in the architecture makes it self-adaptive and driver-specific resulting in better speed prediction.

1) Complexity analysis: the execution time of each methodology is different due to their various architecture and complexity. Ideal (**IDL**) and motion-preserving (**MP**) methodologies do not require any training phase, while the other statistical model-based methodologies (**RF**, **FFNN**, and **NARX**) implement machine learning models that should be trained.

The time needed for the training and prediction phases in each methodology is shown in Table II. It needs to be noted that the training phase is done offline and it is not considered as a bottleneck for the controller. The prediction phase is more important since it is integrated into the controller for energy management. The ideal (**IDL**) and motion-preserving (**MP**) methodologies require inconsiderable time since they implement just one equation. However, the statistical models take more time to predict in the interest of having smaller error for longer-term prediction. The prediction time for NN-based models are the smallest as they implement constant number of equations to predict a value as opposed to random forests (**RF**) which requires traversing through multiple decision trees.

TABLE II
COMPLEXITY OF THE DRIVING BEHAVIOR ESTIMATION.

Methodolgy	Acronym	Context-Aware	Execution Time	
			Training (s)	Prediction (ns)
Ideal	IDL	✗	0.00	0.67
Motion-Preserving	MP	✗	0.00	1.87
Random Forests	RF	✓	3685.17	30923.88
FeedForward Neural Network	FFNN	✓	2459.88	316.90
Nonlinear AutoRegressive with eXogenous Inputs	**NARX**	✓	9240.23	631.10

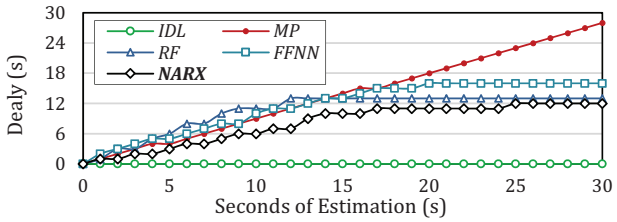

Fig. 7. Estimation delay for different methodologies for various window sizes.

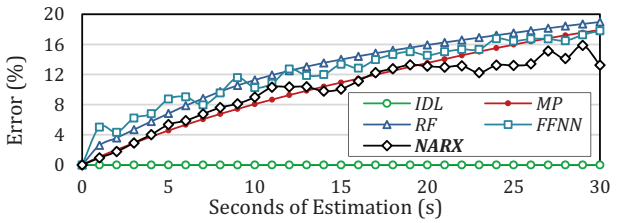

Fig. 8. Estimation error for different methodologies for various window sizes.

2) Estimation accuracy: the accuracy of different methodologies is compared in terms of Mean Absolute Error (*MAE*) and Delay (D). For n-second future vehicle speed prediction, $MAE(n)$ and $D(n)$ are calculated as follows:

$$MAE\ (n) = \frac{1}{M}\sum_{i=1}^{M} |SP_n(i) - S_n(i)| \tag{13}$$

$$D\ (n) = \textbf{argmax}\ \rho\ (\hat{SP}_n, \hat{S}_n) \tag{14}$$

where SP_n is the vector of the estimated n-second future speeds and S_n is the vector of the real speeds during that time. M is the number of samples for validation or test. Function ρ calculates the correlation between the two normalized signals $\hat{SP}_n$ and $\hat{S}_n$. Due to the nature of our control optimization, the value of error in the prediction is not the major factor affecting the output of the optimization and control performance. The more valuable aspect is the model ability to predict the changing trend of the vehicle speed. The model should be able to predict whether the speed is going to increase or decrease. The MAE represents how close the predictions are to the real values, however, it does not show correctness of the

model in predicting the direction and changing trend of speed. Meanwhile, $D\ (n)$ shows the agility of the model to catch up with the changing trend of speed (not execution time). For instance, $D\ (23) = 12$ demonstrates that if a changing trend is going to occur in 23 seconds, it might not be predictable by the model up to 12 seconds (on average) before its occurrence.

Figures 7 and 8 illustrate mean absolute error and delay for the methodologies for n-second ($n = 1 : 30$) future speed prediction. Longer term estimation increases the error except for the ideal (**IDL**) methodology. The error and delay of our novel context-aware methodology (**NARX**) is less than the other methodologies especially for longer estimation ($n > 15$). This is due to the intrinsic feedback in our context-aware NARX enabling self-adaptive model which adjusts to the specific driver behavior resulting in lower delay and estimation error, as opposed to the other statistical models (**RF** and **FFNN**).

3) Optimization cost: the vehicle speed prediction is integrated into the battery lifetime-aware automotive climate control. Hence, the prediction accuracy and delay may influence the MPC optimization and control performance. The optimization cost includes the thermal comfort and battery lifetime costs (Equation 12 in Section III). It has been shown that the optimization cost decreases by having the future EV power requests, compared to the traditional climate control (which only considers the cabin temperature). However, this has been previously done when the real future vehicle speeds were given (**IDL** methodology). The results prove the statements mentioned in Section II-B about the performance of **NARX**; the **NARX** model has smaller prediction time, estimation error, and average delay for the model compared to other models (**RF** and **FFNN**). Hence, in the following, we select our context-aware **NARX** model as the best statistical modeling.

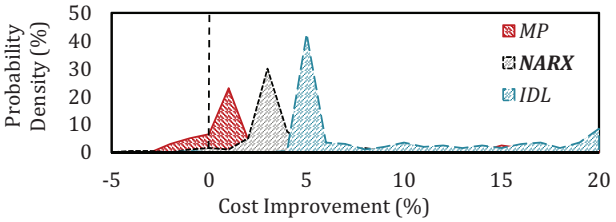

Fig. 9. Distribution of total cost improvement for different methodologies.

Figure 9 shows the distribution of the optimization cost improvement over the traditional climate control. In other words, it shows how these methodologies improve the control quality compared to the the traditional climate control. The ideal (**IDL**) methodology illustrates the maximum improvement 11% (larger mean and smaller variance values). Our context-aware **NARX** can reach up to 6.9% improvement (on average) which is higher than the state-of-the-art methodology of motion-preserving (**MP**). This is mainly achieved because of the lower estimation error and average delay of the model.

4) EV performance: driving range and battery lifetime are the important factors in EVs. Hence, the optimization performance in the battery lifetime-aware climate control is analyzed.

Figure 10 shows the energy saving, battery lifetime (SoH) improvement, and total optimization cost reduction achieved,

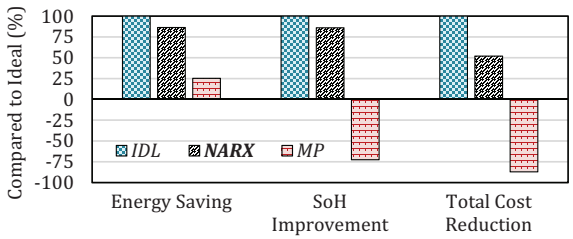

Fig. 10. Energy saving, battery lifetime improvement, and total optimization cost reduction compared to ideal case.

compared to the ideal methodology in percentage. For instance, using **IDL** methodology, the SoC deviation reduced by 11% to improve the battery lifetime. However, using context-aware **NARX** methodology, SoC deviation reduced by 9.5% and there was no improvement in **MP** methodology. It is shown that our context-aware **NARX** can help the battery lifetime-aware automotive climate control to improve the driving range and battery lifetime up to 82% of the maximum improvement achievable (by **IDL** methodology). Small degradation in the improvement is due to the estimation error and misprediction of the future vehicle speeds and EV power requests. However, our context-aware **NARX** methodology is much better than the motion preserving (**MP**) methodology especially in terms of the battery lifetime. The poor performance of the **MP** is due to the fact that it does not capture the uncertainty in driving behavior for long term prediction. Hence, the mispredicted future vehicle speeds and EV power requests cause the energy management to decide wrong control inputs which do not help the performance.

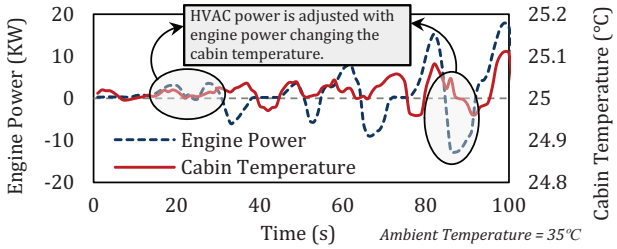

Fig. 11. Temperature variation when integrating the driving behavior estimation into battery lifetime-aware automotive climate control optimization.

5) Thermal comfort: the automotive climate control has been set to maintain the cabin temperature around the target temperature (25°C) with the variation of up to 1°C (≈4%) The ambient temperature is assumed to be 35°C. Since the constraint is very stringent, no thermal comfort degradation has been seen in terms of temperature variation (see Figure 11) compared to the ideal methodology. The figure illustrates how the HVAC power and cabin temperature are adjusted by the climate control according to the estimated EV power requests such that the battery stress is minimized. It needs to be noted that deciding the set points for the cabin temperature (variation of 2°C) is a very costly decision for the climate control in terms of the power consumption required by the HVAC system to maintain that temperature. Therefore, it becomes important for the climate control methodology to exploit the variation of the cabin temperature around the target temperature to improve the battery lifetime and energy consumption.

6) Estimation window: having more knowledge of the future vehicle speeds and EV power requests might help the performance of the battery lifetime-aware automotive climate control. We have analyzed its performance in terms of the optimization cost improvement for different estimation window sizes. We have changed the time step duration and the number of steps in the window size of the prediction horizon:

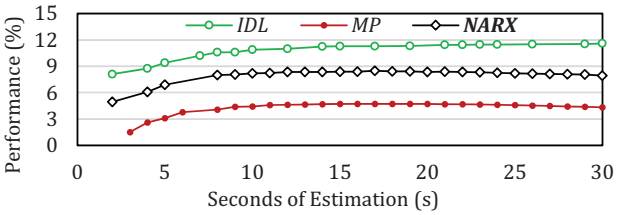

Fig. 12. Impact of estimation window size on the climate control performance.

Figure 12 shows that in **IDL** methodology, the performance (total optimization cost improvement) always increases by having more future information. In other words, longer-term prediction improves the performance of the energy and battery management; it results in more battery lifetime (SoH) improvement and energy saving. In our context-aware **NARX** methodology, the performance also increases for longer predictions, but it saturates after more than 17-second future estimation. This is due to the fact that the estimation error increases for the time instances further away from the immediate present causing the misprediction of the future vehicle speeds and EV power requests. Higher misprediction rate and average delay for the methodologies like motion-preserving (**MP**) result in lower performance compared to our methodology and definitely ideal methodology. That is due to the uncertainty in the driving behavior that will result in poor performance of the controller compared to the **IDL**. The uncertainty is modeled and further eliminated in our context-aware **NARX** model by using average vehicle speed data to represent the route condition.

V. Conclusions

State-of-the-art EV battery and energy managements leverage long-term power prediction to optimize their control inputs and improve the EV driving range and battery lifetime. However, they have only considered the driving route which is not enough for accurate modeling and estimation of the EV power requests. Moreover, the state-of-the-art driving behavior modeling and estimation methodologies focus on short-term prediction and fail to predict for long term. In this paper, we proposed a novel context-aware methodology using NARX architecture to model and estimate the driving behavior in terms of future vehicle speeds for up to 30 seconds. Our methodology shows only 12% estimation error for up to 30-second speed prediction which is improved by 27% compared to the state-of-the-art. Moreover, we showed in our results that our novel context-aware NARX model can help an energy management methodology like a battery lifetime-aware automotive climate control to improve its control performance up to 82% of the maximum performance achievable in the ideal methodology where all the future vehicle speeds are assumed to be known.

References

[1] Jian Cao and Ali Emadi. A New Battery/UltraCapacitor Hybrid Energy Storage System for Electric, Hybrid, and Plug-In Hybrid Electric Vehicles. *IEEE Transactions on Power Electronics*, pages 122–132, 2012.

[2] Martin Lukasiewycz and Sebastian Steinhorst. System Architecture and Software Design for Electric Vehicles. *Proceedings of the Design Automation Conference (DAC'13)*, pages 1–6, 2013.

[3] Alan Millner. Modeling Lithium Ion Battery Degradation in Electric Vehicles. *IEEE Conference on Innovative Technologies for an Efficient and Reliable Electricity Supply*, pages 349–356, 2010.

[4] Yanzhi Wang, Xue Lin, Qing Xie, Naehyuck Chang, and Massoud Pedram. Minimizing State-of-Health Degradation in Hybrid Electrical Energy Storage Systems with Arbitrary Source and Load Profiles. *Design Automation and Test in Europe (DATE)*, pages 1–4, 2014.

[5] Jeremy Neubauer et al. Thru-life impacts of driver aggression, climate, cabin thermal management, and battery thermal management on battery electric vehicle utility. *Journal of Power Sources*, pages 262–275, 2014.

[6] Korosh Vatanparvar, Sina Faezi, Igor Burago, Marco Levorato, and Mohammad Abdullah Al Faruque. Driving Behavior Modeling and Estimation for Battery Optimization in Electric Vehicles: Work-in-progress. *Proceedings of the Twelfth IEEE/ACM/IFIP International Conference on Hardware/Software Codesign and System Synthesis Companion*, pages 15:1–15:2, 2017.

[7] Kiran R. Kambly and Thomas H. Bradley. Estimating the HVAC energy consumption of plug-in electric vehicles. *Journal of Power Sources*, pages 117–124, 2014.

[8] Korosh Vatanparvar and Mohammad Abdullah Al Faruque. Battery Lifetime-Aware Automotive Climate Control for Electric Vehicles. *52nd Annual Design Automation Conference (DAC)*, (37), 2015.

[9] Mohammad Abdullah Al Faruque and Korosh Vatanparvar. Modeling, Analysis, and Optimization of Electric Vehicle HVAC Systems. *Asia and South Pacific Design Automation Conference (ASP-DAC)*, pages 1–6, 2016.

[10] Korosh Vatanparvar and Mohammad Abdullah Al Faruque. Path to Eco-Driving: Electric Vehicle HVAC and Route Joint Optimization. *IEEE Design & Test*, 2017.

[11] Korosh Vatanparvar and Mohammad Abdullah Al Faruque. OTEM: Optimized Thermal and Energy Management for Hybrid Electrical Energy Storage in Electric Vehicles. *Conference on Design, Automation & Test in Europe (DATE)*, pages 1–6, 2016.

[12] Habiballah Rahimi-Eichi, Unnati Ojha, et al. Battery Management System: An Overview of Its Application in the Smart Grid and Electric Vehicles. *IEEE Industrial Electronics Magazine*, pages 4–16, 2013.

[13] Yanzhi Wang, Xue Lin, Massoud Pedram, and Naehyuck Chang. Joint Automatic Control of the Powertrain and Auxiliary Systems to Enhance the Electromobility in Hybrid Electric Vehicles. *Proceedings of the Design Automation Conference (DAC'15)*, pages 1–6, 2015.

[14] Xue Lin, Paul Bogdan, Naehyuck Chang, and Massoud Pedram. Machine Learning-Based Energy Management in a Hybrid Electric Vehicle to Minimize Total Operating Cost. *IEEE/ACM International Conference on Computer-Aided Design (ICCAD)*, pages 627–634, 2015.

[15] Yan Wang et al. Context-Aware and Energy-Driven Route Optimization for Fully Electric Vehicles via Crowdsourcing. *IEEE Transactions on Intellogent Transportaion Systems*, pages 1331–1345, 2013.

[16] Korosh Vatanparvar, Jiang Wan, and Mohammad Abdullah Al Faruque. Battery-Aware Energy-Optimal Electric Vehicle Driving Management. *International Symposium on Low Power Electronics and Design (ISLPED)*, pages 353–358, 2015.

[17] Korosh Vatanparvar and Mohammad Abdullah Al Faruque. Electric Vehicle Optimized Charge and Drive Management. *ACM Transaction on Design Automation of Electronic Systems (TODAES)*, 2017.

[18] Korosh Vatanparvar and Mohammad Abdullah Al Faruque. Eco-Friendly Automotive Climate Control and Navigation System for Electric Vehicles. *International Conference on Cyber-Physical Systems (ICCPS)*, pages 1–10, 2016.

[19] Thomas Levermore et al. A Review of Driver Modelling. *UKACC International Conference on Control (CONTROL)*, pages 296–300, 2014.

[20] Stéphanie Lefèvre, Dizan Vasquez, and Christian Laugier. A survey on motion prediction and risk assessment for intelligent vehicles. *Robomech Journal*, 1(1):1, 2014.

[21] Heikki Summala. Brake Reaction Times and Driver Behavior Analysis. *Transportation Human Factors*, 2(3):217–226, 2000.

[22] Maral Amir and Tony Givargis. Hybrid state machine model for fast model predictive control: Application to path tracking. *International Conference on Design (ICCAD)*, pages 185–192, 2017.

[23] Ashesh Jain, Hema S Koppula, Shane Soh, Bharad Raghavan, Avi Singh, and Ashutosh Saxena. Brain4Cars: Car That Knows Before You Do via Sensory-Fusion Deep Learning Architecture. *arXiv preprint arXiv:1601.00740*, 2016.

[24] Amardeep Sathyanarayana, Pinar Boyraz, et al. Driver Behavior Analysis and Route Recognition by Hidden Markov Models. *International Conference on Vehicular Electronics and Safety (ICVES)*, pages 276–281, 2008.

[25] Sei-Wang Chen, Chiung-Yao Fang, and Chih-Ting Tien. Driving behaviour modelling system based on graph construction. *Transportation research part C: emerging technologies*, 26:314–330, 2013.

[26] José Maria P Menezes and Guilherme A Barreto. Long-term time series prediction with the NARX network: An empirical evaluation. *Neurocomputing*, 71(16):3335–3343, 2008.

[27] Hava T Siegelmann et al. Computational Capabilities of Recurrent NARX Neural Networks. *IEEE Transactions on Systems, Man, and Cybernetics, Part B: Cybernetics*, 27(2):208–215, 1997.

[28] Konrad Reif. Fundamentals of Automotive and Engine Technology. *Springer: Bosch professional automotive information*, 2014.

[29] Srdjan M Lukic et al. Effects of Drivetrain Hybridization on Fuel Economy and Dynamic Performance of Parallel Hybrid Electric Vehicles. *IEEE Transactions on Vehicular Technology*, pages 385–389, 2004.

[30] Mounir Zeraoulia, Mohamed El Hachemi Benbouzid, and Demba Diallo. Electric Motor Drive Selection Issues for HEV Propulsion Systems: A Comparative Study. *IEEE Transactions on Vehicular Technology*, pages 1756–1764, 2006.

[31] K. David Huang, Sheng Chung Tzeng, Tzer Ming Jeng, and Wing Ding Chiang. Air-conditioning system of an intelligent vehicle-cabin. *Applied Energy*, pages 545–557, 2006.

[32] John Wang, Ping Liu, Jocelyn Hicks-Garner, et al. Cycle-life model for graphite-LiFePO4 cells. *Journal of Power Sources*, 2011.

[33] Dennis Doerffel and Suleiman Abu Sharkh. A critical review of using the Peukert equation for determining the remaining capacity of lead-acid and lithium-ion batteries. *Journal of Power Sources*, pages 395–400, 2006.

[34] Li Sun, Kaiwu Feng, Chris Chapman, and Nong Zhang. An Adaptive Power Split Strategy for Battery-Supercapacitor Powertrain Design, Simulation and Experiment . *IEEE Transactions on Power Electronics*, 2017.

[35] Aris Polychronopoulos, Manolis Tsogas, et al. Sensor Fusion for Predicting Vehicles' Path for Collision Avoidance Systems. *IEEE Transactions on Intelligent Transportation Systems*, pages 549–562, 2007.

[36] Google. Google API Web Services, 2017.

[37] Leo Breiman. Random Forests. *Machine learning*, 45(1):5–32, 2001.

[38] B Yegnanarayana. *Artificial Neural Networks*. PHI Learning Pvt. Ltd., 2009.

[39] Robert R Andrawis et al. Forecast combinations of computational intelligence and linear models for the NN5 time series forecasting competition. *International Journal of Forecasting*, 27:672–688, 2011.

[40] Martin Fodslette Møller. A Scaled Conjugate Gradient Algorithm for Fast Supervised Learning. *Neural networks*, 6(4):525–533, 1993.

[41] Transportation Research Board of the National Academy of Sciences. The 2nd Strategic Highway Research Program Naturalistic Driving Study Dataset. Available from the SHRP 2 NDS InSight Data Dissemination, 2013.

Korosh Vatanparvar (GSM'14) is currently a senior Ph.D. candidate from AICPS Lab. in Electrical Engineering and Computer Science Dept. at University of California, Irvine. He received his B.Sc. degree in Electrical Engineering from Sharif University of Technology in 2013. He obtained his M.Sc. degree in Electrical and Computer Engineering from University of California, Irvine in 2015. He has received two best paper awards in DAC 2015 and DATE 2016 conferences and has been nominated for best paper award in ICCAD 2017. His research is mainly focused on Cyber-Physical Systems, Embedded Systems, Design Automation, Model-Based Design, Internet-of-Things for reliability, energy efficiency, and security. He is a graduate student member of IEEE and ACM.

Sina Faezi has received his B.Sc. degree in electrical engineering from Sharif University of Technology in 2015 and his M.S. degree in computer engineer from University of California, Irvine (UCI) in 2017. He is currently working toward his Ph.D. degree in computer engineering at University of California, Irvine in AICPS Lab. His research interests include data-driven modeling for cyber-physical systems, machine learning, and statistical models.

Igor Burago obtained the B.S. degree in Applied Mathematics and Informatics summa cum laude from the Far Eastern Federal University, Russia, in 2011, and the M.S. degree in Computer and Information Science from the University of Oregon in 2014. He is currently a fourth-year Ph.D. student in the Department of Computer Science at the University of California, Irvine.

Marco Levorato (S'06-M'09) received the B.S. and M.S. degrees in electrical engineering summa cum laude from the University of Ferrara, Italy, in 2005 and 2003, respectively, and the Ph.D. degree in electrical engineering from the University of Padova, Italy, in 2009. He is currently an Assistant Professor in Computer Science with the University of California at Irvine. He has post-doctoral appointments with Stanford University, the University of Southern California, and the Royal Institute of Technology in Stockholm, Sweden. He is a recipient of a best paper award from the IEEE Globecom 2012, the UC Hellman Foundation Award, and has been twice nominated for the Best Young Researcher Award, Department of Information Engineering, University of Padova, Italy.

Mohammad Al Faruque is currently with the University of California Irvine (UCI), where he is an associate professor (with tenure) and directing the Cyber-Physical Systems Lab. Prof. Al Faruque is the recipient of the IEEE CEDA Ernest S. Kuh Early Career Award 2016. He is also the recipient of the UCI Academic Senate Distinguished Early-Career Faculty Award for Research 2017 and the School of Engineering Early-Career Faculty Award for Research 2017. He served as an Emulex Career Development Chair during October 2012 till July 2015. Before, he was with Siemens Corporate Research and Technology in Princeton, NJ. His current research is focused on system-level design of embedded systems and Cyber-Physical-Systems (CPS) with special interest on model-based design, multi-core systems, CPS security, etc. Prof. Al Faruque received his B.Sc. degree in Computer Science and Engineering (CSE) from Bangladesh University of Engineering and Technology (BUET) in 2002, and M.Sc. and Ph.D. degrees in Computer Science from Aachen Technical University and Karlsruhe Institute of Technology, Germany in 2004 and 2009, respectively. Prof. Al Faruque received the Thomas Alva Edison Patent Award 2016 from the Edison foundation, the 2016 DATE Best Paper Award, the 2015 DAC Best Paper Award, the 2009 IEEE/ACM William J. McCalla ICCAD Best Paper Award, the 2016 NDSS Distinguished Poster Award, the 2008 HiPEAC Paper Award, the 2015 Hellman Fellow Award, the 2015 Kane Kim Fellowship Award, the 2017 DAC Best Paper Award Nomination, the 2017 ICCAD Best Paper Award Nomination, the 2012 DATE Best IP Award Nomination, the 2005 DAC Best Paper Award Nomination, the EECS Professor of the year 2015-16 Award, and the 2015 UCI Chancellors Award for Excellence in Fostering Undergraduate Research. Besides 80+ IEEE/ACM publications in the premier journals and conferences, Prof. Al Faruque holds 6 US patents.